Method for multi-spectral tomographic reconstruction
of chlorophyll concentration for ocean water

Roberto Pinto Souto[1]
Fabiana Ferreira Paes [1]
Haroldo Fraga de Campos Velho[1]
Stephan Stephany[1]
Airam Jônatas Preto[1]
Andrea Schwertner Charão[2]
Juliana Kaiser Vizzotto[3]
Philippe Olivier Alexandre Navaux[4]
Nicolas Maillard[4]

[1] Instituto Nacional de Pesquisas Espaciais – INPE
Av. dos Astronautas, 1758 – 12227-010 – São José dos Campos - SP, Brasil
rp.souto@gmail.com, {fabiana.paes, haroldo, stephan, airam}@lac.inpe.br

[2] Universidade Federal de Santa Maria – UFSM
Inst. de Informática – Av Roraima, 1000 – CEP 97105-900 – Santa Maria - RS, Brasil
andrea@inf.ufsm.br

[3] Centro Universitário Franciscano – UNIFRA
Rua dos Andradas, 1614 – CEP 97010-032 – Santa Maria
juvizzotto@gmail.com

[4] Universidade Federal do Rio Grande do Sul – UFRGS
Inst. de Informática – Caixa Postal 15064 – CEP 91501-970 – Porto Alegre - RS, Brasil
{navaux, nicolas}@inf.ufrgs.br

Abstract.   Based on the water-leaving multi-spectral radiance from the ocean water, the 3D chlorophyll concentration is reconstructed. The inverse problem is formulated as an optimization problem and iteratively solved by the meta-heuristics Ant Colony Optimization, using the radiative transfer equation as direct model. An objective function is given by the square difference between computed and experimental radiance at every iteration. It was included an intrinsic regularization scheme that pre-selects candidate solutions at every iteration based on their smoothness, quantified by the 2nd order Tikhonov norm. Additional information is also used to compute the inverse solution: the concavity of the chlorophyll profile that is verified by means of its second derivative. In the higher depths a additional step was necessary to improve the reconstruction, since it is usually obtained poor results in this region for most of the profiles, since we are considering only data of raciances measured above the water. For considering an ocean surface divided in several sub-domains (as pixels in an image), there will be a significant amount of computation to be performed. The demand for high processing power is addressed with the use of grid computing to speed up the inversion process. A grid infrastructure with three clusters geographically distributed was built to perform the inversion for each pixel.

Keywords: hydrologic optics, inverse problems, remote sensing ótica hidrológica, problemas inversos, sensoriamento remoto.

1. Introduction

The direct or forward radiative transfer problem in hydrologic optics, in the steady state, involves the determination of the radiance distribution in a body of water, given the boundary conditions, source term, inherent optical properties (IOPs), as the absorption and scattering coefficients, and the phase function. The inverse radiative transfer problem arises when physical properties, internal light sources and/or boundary conditions must be estimated from

radiometric measurements of the underwater light field. A challenge in the inverse hydrologic optics problem is to determine the IOPs, only considering water-leaving radiance.

The inverse problem is formulated as an optimization problem and iteratively solved using a intrinsic regularization scheme (PRETO et al., 2004; SOUTO et al., 2004) coupled to a standard Ant Colony Optimization (ACO) (DORIGO; MANIEZZO; COLORNI, 1996). The regularization scheme pre-selects candidate solutions based on their smoothness, quantified by a Tikhonov norm (PRETO et al., 2004). Profiles generated with wrong curvature are filtering out by a second derivative criterion (SOUTO et al., 2007b).

An objective function is given by the square difference between computed and experimental radiances at every iteration. Each candidate solution corresponds to a discrete chlorophyll profile. The chlorophyll profile is reconstructed from multi-spectral water-leaving radiances of ocean surface, following the methodology presented by Chalhoub and Campos Velho (CHALHOUB; VELHO, 2003).

This inverse procedure is a computing intensive. But, such scheme is just one satellite pixel. For a ocean surface observed by a satellite, the image contains many pixels, and in general we are interested to compute a 3D tomography from a frame of images. Due to the nature of reconstruction, each pixel inversion is independent from the inversion of other pixels. This constitutes in a good challenge addressed by grid computing approach. A grid infrastructure was built to perform the inversion for each pixel, managing a queue of independent jobs submitted to three clusters geographically distributed.

This paper is organized as follows: section 2 introduces the basic nomenclature and equations governing light transmission in natural water. Section 3 focuses on the relationship between IOPs and chlorophyll concentration. In section 4, we present the Ant Colony Optimization method employed in our experiments. The inversion scheme is presented in section 5 and the tomographic reconstruction using grid computing is discusses in section 6. The final section presents our conclusions and suggestions for future work.

2. Light transmission in natural water

The radiative transfer equation (RTE) models the transport of photons through a medium (GORDON, 1984). Light intensity is given by a directional quantity, the radiance L, that measures the rate of energy being transported at a given point and in a given direction. For a given horizontal plane, this direction is defined by a polar angle θ (relative to the normal of the plane) and a azimuthal angle φ (a possible direction in that plane). At any point of the medium, light can be absorbed, scattered or transmitted, according to the absorption (a) and scattering (b) coefficients and to a scattering phase function that models how light is scattered in any direction. An attenuation coefficient c is defined as $c = a + b$ and the geometrical depth is mapped to a optical depth τ that embeds c.

Assuming a plane-parallel geometry, for the case of azimuthal symmetry (no dependence on j), isotropic medium and absence of source term, the one dimensional integro-differential RTE, can be written as:

$$\mu \frac{d}{d\tau} L_{r,\lambda}(\tau,\mu) + L_{r,\lambda}(\tau,\mu) = \frac{\varpi_r(\lambda)}{2} \int_{-1}^{1} L_{r,\lambda}(\tau,\mu) d\mu' \tag{1}$$

with

$$\varpi_r(\lambda) = \frac{b_r(\lambda)}{c_r(\lambda)} = \frac{b_r(\lambda)}{a_r(\lambda) + b_r(\lambda)} \tag{2}$$

for $r = 1, 2, \ldots, R$ and $\mu \in (0, 1]$, a heterogeneous medium is modeled as a set of R

homogeneous finite layers. Optical variable τ is discretized in $R + 1$ values, varying from $\tau_0 = 0$ up to $\tau_R = \zeta$, where ζ is the medium *optical depth*, constant in the region r, for any value of τ, where $c_r(\lambda)$, $a_r(\lambda)$ and $b_r(\lambda)$ are respectively the attenuation, the absorption and the scattering coefficients, for a given wavelength λ.

Equation (1) is subject to boundary conditions

$$L_{1,\lambda}(\tau_0, \mu) = L_{R,\lambda}(\tau_R, -\mu) = 0 \tag{3}$$

and for the region interfaces in $r = 1, 2, \ldots, R - 1$, is assumed the continuity of the radiance.

$$L_{r,\lambda}(\tau_r, \pm\mu) = L_{r+1,\lambda}(\tau_r, \pm\mu) \tag{4}$$

for $\mu \in (0, 1]$. In this work, the RTE was solved by the LTS$_N$ method (BARICHELLO; VILHENA, 1993).

3. The chlorophyll and IOPs relationship

Bio-optical models are employed in this work to correlate the absorption and scattering coefficients to the chlorophyll concentration. These coefficients are assumed to be constant in each region. Therefore discrete values a_r and b_r can be estimated for each region from the discrete values C_r.

Usually, chlorophyll profiles can be represented according to Gaussian distributions (MOBLEY, 1994):

$$C(z) = C_{bg} + \frac{h}{\sigma\sqrt{2\pi}} \exp\left[-\frac{1}{2}\left(\frac{z - z_{max}}{\sigma}\right)^2\right] \tag{5}$$

where z is the depth in meters and $C(z)$ is given in mg/m^3. This profile can be seen in results section of this work, termed *exact*. A bio-optical model was formulated by Morel (GORDON, 1984) for the absorption coefficient,

$$a_r(\lambda) = [a^w + 0.06a^c C_r^{0.65}][1 + 0.2e^{-0.014(\lambda-440)}] \tag{6}$$

where a^w is the pure water absorption and a^c is a non dimensional, statistically derived chlorophyll specific absorption coefficient, and λ is the considered wavelength, while another chlorophyll correlation was formulated by Gordon and Morel (MOBLEY, 1994) for the scattering coefficient,

$$b_r(\lambda) = \left(\frac{550}{\lambda}\right)0.30C_r^{0.62} \tag{7}$$

4. Ant colony optimization

The Ant Colony Optimization (ACO) is a method based on the collective behavior of ants choosing the shortest path between the nest and the food source. Each ant marks its path with an amount of pheromone and the marked path is further employed by other ants as a reference.

In the ACO optimization method, several generations of ants are produced. For each generation, a fixed amount of ants (na) is evaluated. Each ant is associated to a feasible path and this path represents a candidate solution, being composed of a particular set of edges of the graph that contains all possible solutions. Each ant is generated by choosing these edges on a probabilistic basis.

A solution is composed of linking ns nodes and in order to connect each pair of nodes, np discrete values can be chosen. This approach was used to deal with a continuous domain.

Therefore, there are $ns \times np$ possible paths $[i, j]$ available. Denoting by ρ the pheromone decay rate, the amount of pheromone T_{ij} at generation t is given by:

$$T_{ij}(t) = (1 - \rho) \cdot T_{ij}(t - 1) \quad t = 1, 2, \ldots, mit \tag{8}$$

where mit is the maximum number of iterations.

The best ant of each generation is then chosen and it is allowed to mark with pheromone its path. This will influence the creation of ants in the further generations. The pheromone put by the ants decays due to an evaporation rate. Finally, at the end of all generations, the best solution is assumed to be achieved.

5. Inversion scheme

The inverse problem is formulated according to an implicit approach, leading to an optimization problem (LAMM, 1993). The algorithm is expressed as a constrained nonlinear optimization problem, in which the direct problem is iteratively solved for successive approximations of the unknown parameters. Iteration proceeds until an objective-function, representing the least-square fit of model results and experimental data added to a regularization term, converges to a specified small value.

The set of parameters to be estimated is $R + 1$ discrete values of the chlorophyll concentration C_r, for $r = 0, 1, \ldots, R$ at optical depths τ_r taken at the upper interface of the regions. Experimental data are the discrete radiances $L^{\exp}(\tau_0, \mu_i, \lambda_j)$ for $i = 1, 2, \ldots, \frac{N_\mu}{2}$ and $j = 1, 2, \ldots, N_\lambda$. Therefore, the $R + 1$ discrete values of the concentration are estimated from $\frac{N_\mu}{2} \times N_\lambda$ spectral radiance values right above of sea surface. The objective function $J(C)$ is given by the square difference between experimental and model radiances plus a regularization term.

$$
\begin{aligned}
J(C) &= \sum_{i=1}^{N_\mu/2} \sum_{j=1}^{N_\lambda} [L^{\exp}(\tau_0, -\mu_i, \lambda_j) - L_C(\tau_0, -\mu_i, \lambda_j)]^2 \\
&+ \gamma \Gamma(C)
\end{aligned}
\tag{9}
$$

where $\Gamma(C)$ is the regularization function, that is weighted by a regularization parameter γ. For instance, the 2nd order Tikhonov regularization (TIKHONOV; ARSENIN, 1977) is defined by

$$\Gamma(C) = \sum_{r=0}^{R-2} (C_r - 2C_{r+1} + C_{r+2})^2 \tag{10}$$

5.1. Intrinsic Regularization and Concavity criterion

In the current work, a ACO-based inverse solver with an intrinsic regularization scheme (PRETO et al., 2004) is employed without the regularization term ($\gamma = 0$) shown in Equation (9).

As a smooth profile is required, this is a known information about the inverse solution. Such knowledge is included in the generation of the candidate solutions by means of pre-selecting the smoother ants according to the 2nd order Tikhonov norm. Actually, a kind of pre-regularization is performed. Therefore the usual regularization term is not required

Besides the smoothness, additional information is also used to compute the inverse solution: the concavity of the chlorophyll profile that is verified by means of its second derivative (SOUTO et al., 2007b). Since only curves with negative concavity are expected, a penalty is assigned to

profiles with positive concavity. For each of these profiles, an overhead value is added to the evaluated objective function (Equation 9).

6. Chlorophyll concentration: tomographic reconstruction using grid computing

In this work, we simulate a specific case with dimension of 60 km × 60 km, and 40 meters of depth for the ocean spatial domain. The horizontal domain is uniformly divided in 36 smaller regions of 10 km × 10 km.

There are three profiles to be recovered in the whole domain. Each profile was generated employing the Gaussian model given by the Equation 5, and the used parameters to construct each profile, are showed in Table 1.

Table 1: Parameters of Gaussian chlorophyll profiles for Equation 5

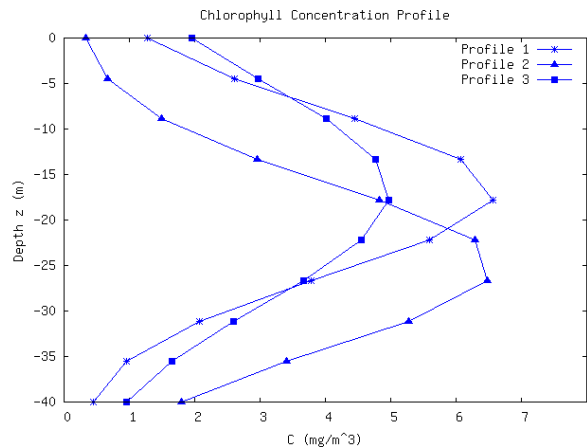| Profile	C_{bg}	h	σ	z_{max}
1	0.2	144.0	9.0	17.0
2	0.2	144.0	9.0	25.0
3	0.2	144.0	12.0	17.0

Figure 1: Chlorophyll concentration profiles according parameters of Table 1.

The profile distribution is shown in Figure 2. As one can note, there are 20 sub-regions with profile-1, 12 with profile-3 and 4 sub-regions which correspond to profile-2.

For each profile there is a set of radiance multi-spectral values which come from the ocean surface. It was added a random noise of 1% in the radiance values of all regions. Each region with the same profile has a different initial random sequence of noise values, i.e., a different seed sequence.

It is supposed a good estimation was obtained up to the peak of the curve (average profile) with poorer agreement to the lower part of the profile (depth below to the peak – see Figure 3). In order to improve the inverse solution, a two-step strategy is used: ***step-1*** – the estimation has already performed for the whole profile, and then, in ***step-2***, the reconstruction is carried out only for the lower part of the curve. In the *step-2*, each ant is still related to the whole profile, but the values obtained in the *step-1* for the upper part of the water layer are frozen. In other words, *step-2* is a new inverse problem, but simpler than original problem, because *step-2* problem has a lower dimension and a good first guess (obtained in *step-1*).

P1	P1	P1	P1	P1	P1
P1	P3	P3	P3	P3	P1
P1	P3	P2	P2	P3	P1
P1	P3	P2	P2	P3	P1
P1	P3	P3	P3	P3	P1
P1	P1	P1	P1	P1	P1

Figure 2: Profiles distribution in a spatial domain, splitted in 36 regions of 10km × 10km.

(a)   (b)
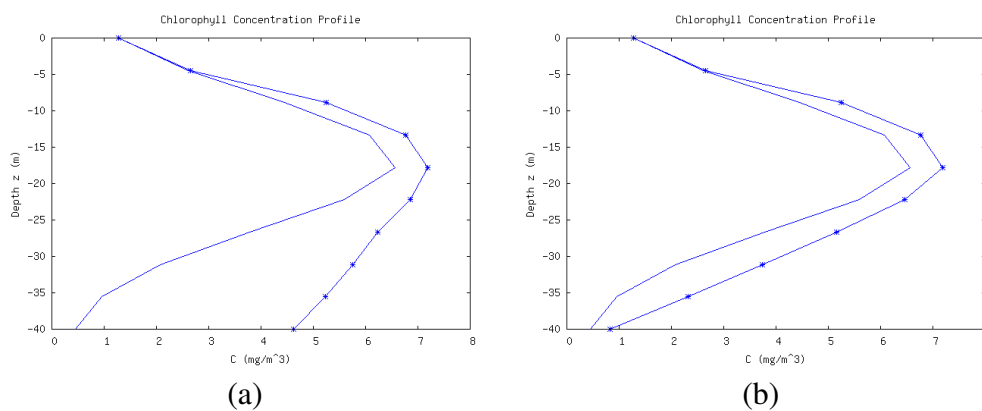
Figure 3: Example of chlorophyll concentration recovering: (a) step-1, (b) step-2.

In each region, the inverse problem of recovering chlorophyll concentration profile, based on the water-leaving radiances must be solved. As these profile reconstructions are independent each other, the set of inversions are treated here as a "Bag-of-Task" application, i.e., a fully independent set of tasks.

Therefore, a parallel computing environment is used to perform the inversion for the entire spatial domain. It was performed a total of 56 jobs, where 36 are regarding to step-1 profiles recovering, and 20 jobs is concerning the step-2 reconstruction for only the profile-1. The jobs are assigned each pixel on the ocean surface (a sub-domain), vectorizing the radiances associated to each pixel, and preparing them to the inversion procedure. The process starts for the execution of the procedure, where a script provides the jobs to the computational system.

Three computer clusters from different institutions were employed: at UFSM, UFRGS and INPE, respectively placed in Santa Maria, Porto Alegre, and São José dos Campos cities. The OurGrid (CIRNE et al., 2005) middleware was used in our tomographic reconstruction. This middleware is targeted to grid computing with "Bag-of-Task" applications. It is a similar grid infrastructure had already employed by these organizations, in other to perform a meso-scale climatology (SOUTO et al., 2007a).

6.1. Ocean chlorophyll tomography

The inverse solver was tested for a multi-region ($R = 9$) offshore ocean water radiative transfer problem with azimuthal symmetry, using multi-spectral radiance data, with a 1% random noise. This data is related to the emerging radiances at the water surface and include
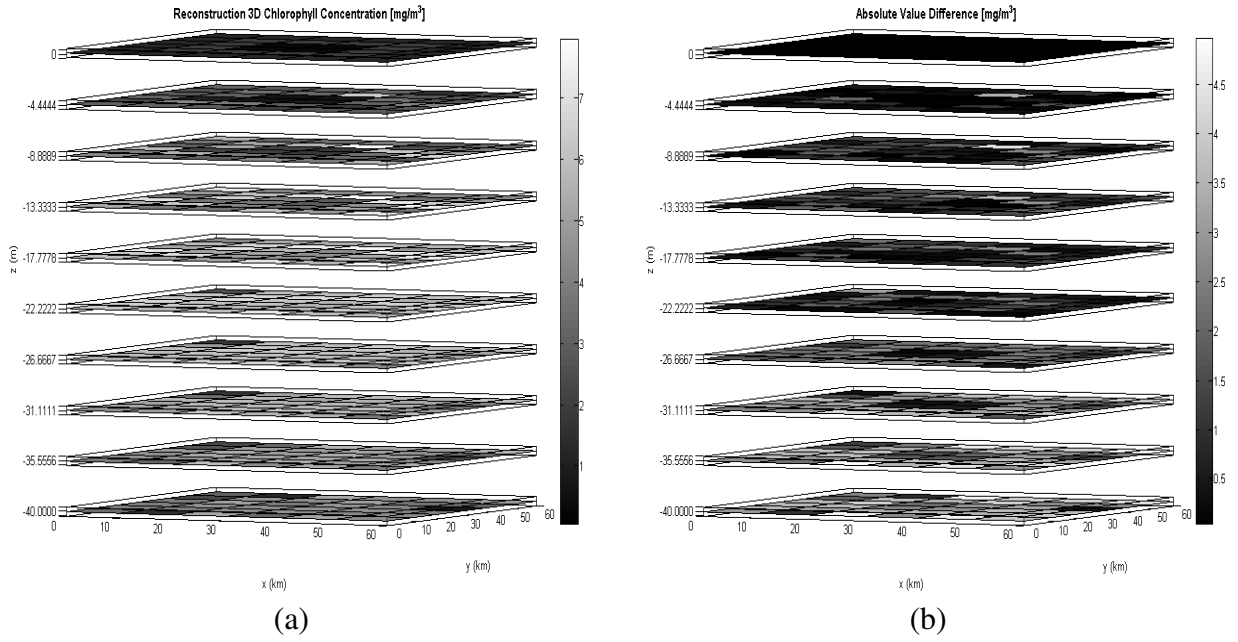
Figure 4: Chlorophyll concentration: (a) estimated, (b) absolute error with the real value.

$N_\mu/2 = 10$ polar directions for each of the $N_\lambda = 10$ wavelengths. In the considered test cases, synthetic data was used to simulate the experimental values.

The ACO implementation required adjustment of parameters as the pheromone decay rate (ρ) and q_0, used in the roulette scheme. Here $\rho = 0.03$ and $q_0 = 0$ were used. A faster convergence is obtained for higher values of ρ, but the inverse solution is not good. There are other parameters in the process, such as the number of possible paths (np) between each pair of the ns nodes, the number of ants na, or the maximum number of iterations mit. These values are shown in Table 2, and they are used for the test cases.

The ACO was executed using na=360 and pre-selecting 1/30 of these ants (na_p=12) according to their smoothness. The range of search for the chlorophyll concentration vary from 0.0003 (1.0/3000.0) up to 10.0 (3000.0/300.0).

Table 2: Seeds and ACO parameters

Seeds (10)	3, 15, 21, 31, 45, 63, 77, 81, 95, 99						
ACO parameters	ns	np	na	na_p	mit	ρ	q0
	10	3000	360	12	400	0.03	0.0

Figure 4(a) shows the reconstructed 3D chlorophyll concentration depicted for 2D 36×36-pixel slices at several depths, while Figure 4(b) shows the absolute error (difference between reconstructed and real values) also for 2D 36×36-pixel slices at the same depths. In both figures the grayscale varies from lower (black) up to higher (white) values.

It can be observed that, in general, for higher depths the correctness of the recovered profiles is decreased. Indeed, once it is used only water-leaving spectral radiances, there is few information coming from the bottom of the spatial domain. However, with the two-step strategy described previously in this section, this effect could be partially reduced.

7. Conclusion

In this work, it was tested the feasibility of recovering different kinds of chlorophyll profiles, in a given spatial domain in the ocean. According the overall estimation of chlorophyll concentration, it indicates that a good reconstruction is usually reached up to half of the domain depth. The intrinsic regularization combined with the concavity criterion, was determinant to obtain such results. However, for the lower half of chlorophyll concentration profiles, the 2-step strategy was necessary to improve the results.

This application was very suitable to perform by using grid computing. Although in this work it have been employed an isotropic model of radiative transfer, em true real cases there is a high degree of anisotropy evolved. It implies in a much higher computational effort to solve the direct problem. Therefore, in this scenario, the grid computing is a feasible alternative to perform this problem.

As future work, we intend to make reconstruction for higher grades of anisotropy, and also for a greater horizontal domain, using a grid environment with more machines to increase the available performance.

References

BARICHELLO, L.; VILHENA, M. A general approach to one-group one-dimensional transport equation. *Kerntechnik*, v. 58, p. 182, 1993.

CHALHOUB, E. S.; VELHO, H. F. de C. Multispectral reconstruction of bioluminescence term in natural waters. *Appl. Numer. Math.*, Elsevier Science Publishers B. V., Amsterdam, The Netherlands, The Netherlands, v. 47, n. 3-4, p. 365–376, 2003. ISSN 0168-9274.

CIRNE, W. et al. Hpc: Paradigm and infrastructure. In: ____. [S.l.]: John Wiley and Sons, 2005. cap. Building a user-level grid for bag-of-tasks applications.

DORIGO, M.; MANIEZZO, V.; COLORNI, A. The ant optimization: optimization by a colony of cooperating agents. *IEEE Trans. Syst. Man Cybernet.-Part B*, v. 26, p. 29, 1996.

GORDON, H. Remote sensing marine bioluminescence: the role of the in-water scalar irradiance. *Applied Optics*, v. 24, p. 1694, 1984.

LAMM, P. Inverse problems and ill-posedness. *Inverse Problems in Engineering: Theory and Practice*, Palm Coast, p. 1–10, 1993.

MOBLEY, C. *Light and Water: Radiative Transfer in Natural Waters*. [S.l.]: Academic Press, 1994. 592 p.

PRETO, A. et al. A new regularization technique for an ant-colony based inverse solver applied to a crystal growth problem. In: UNIVERSITY OF CINCINNATI. *13th Inverse Problem in Engineering Seminar (IPES-2004)*. Ohio, USA, 147, 2004.

SOUTO, R. et al. Processing mesoscale climatology in a grid environment. In: *Seventh IEEE International Symposium on Cluster Computing and the Grid (CCGrid-2007)*. Washington, DC, USA: IEEE Computer Society, 2007. p. 363–370. ISBN 0-7695-1919-9.

SOUTO, R. et al. Determining chlorophill concentration in off-shore sea water from multi-spectral radiances by using second devirtive criterion and ant colony meta-heuristic. In: *Inverse Problems, Design and Optimization Symposium IPDO-2007*. Miami, USA: [s.n.], 2007. v. 1, p. 341–348.

SOUTO, R. P. et al. Reconstruction of chlorophyll concentration profile in offshore ocean water using a parallel ant colony code. In: *Hybrid Metaheuristics*. [S.l.: s.n.], 2004. p. 19–24.

TIKHONOV, A.; ARSENIN, V. *Solutions of Ill-Posed Problems*. Washington: Winston and Sons, 1977.